Structures and energies of vacancy-Cu clusters in α-Fe

A. Takahashi
Department of Quantum Engineering and Systems Science, University of Tokyo, 7-3-1 Hongo, Bunkyo-ku, Tokyo 113-8656, Japan

N. Soneda
Central Research Institute of Electric Power Industry, 2-11-1, Iwado-kita, Komae-shi, Tokyo 201-8511, Japan
and Department of Quantum Engineering and Systems Science, University of Tokyo, 7-3-1 Hongo, Bunkyo-ku, Tokyo 113-8656, Japan

S. Ishino
Department of Applied Science, Tokai University, 1117, Kitakaname, Hiratsuka-shi, Kanagawa 259-1292, Japan

G. Yagawa
Department of Quantum Engineering and Systems Science, University of Tokyo, 7-3-1 Hongo, Bunkyo-ku, Tokyo 113-8656, Japan
(Received 29 January 2002; revised manuscript received 30 October 2002; published 16 January 2003)

We study structures and energies of vacancy-Cu clusters in α-Fe, which provide fundamental information for understanding the mechanism of neutron-irradiation embrittlement of nuclear reactor pressure vessel materials. Extensive molecular-dynamics (MD) and Monte Carlo computer simulations with the use of the embedded atom method (EAM) potential for the Fe-Cu system are performed to obtain energy-minimum structures of vacancy-Cu clusters of various sizes in a α-Fe matrix. We find that, in general, a vacancy-Cu cluster consists of a vacancy cluster buried at the center of a Cu shell. The formation energies for the vacancy-Cu clusters are calculated from the MD results, and we develop an equation describing the formation energy as a function of the numbers of vacancies and Cu atoms. We find that the number of Cu atoms on the surface of the vacancy cluster plays an important role in determining the formation energy of the vacancy-Cu clusters. The binding energies of a vacancy and a Cu atom to the vacancy-Cu clusters are also calculated. We find that the interaction between vacancies and Cu atoms enhances the binding of the vacancy-Cu clusters.

DOI: 10.1103/PhysRevB.67.024104 PACS number(s): 61.72.Ji, 61.82.Bg

I. INTRODUCTION

Understanding the mechanism of neutron irradiation embrittlement of nuclear reactor pressure vessel (RPV) materials is very important for ensuring the structural integrity of the RPVs in aging nuclear power plants. The embrittlement is primarily caused by the irradiation-induced lattice defects and solute clusters.[1] Especially, Cu-enriched solute clusters are assumed to act as obstacles to dislocation motion and cause irradiation hardening. Many experimental studies have been performed to characterize the nature of such Cu-enriched clusters in neutron-irradiated RPV materials and Fe-Cu model alloys. One of the recent topics is the role of the vacancies in Cu-enriched clusters in terms of the morphology of the Cu-enriched clusters and the binding of Cu atoms and vacancies.

Regarding the morphology of the Cu-enriched clusters, the three-dimensional atom probe technique allows us to observe the clustering of solute and impurity atoms directly in an atomistic length scale.[2–4] A common observation is that the clusters induced by neutron irradiation have very diffuse morphology, and a very large fraction, approximately 50%, of Fe atoms is contained within the clusters. Positron annihilation experiments also provide very important information about the Cu clustering. The coincidence Doppler broadening measurements of the positron annihilation experiments suggest that irradiation-induced Cu clusters should contain vacancies, and such vacancies form a small cluster whose surface is coated by the Cu atoms when the Cu content is as high as $\sim$0.3 wt %.[5]

On the other hand, regarding the binding of Cu atoms and vacancies, the thermal stability of vacancy-type defects containing Cu atoms at the RPV operating temperature of $\sim$300 °C is also of interest. Since the stage-V temperature of pure Fe is below 300 °C, a small vacancy cluster of $\sim$10 vacancies in size cannot survive annihilation.[6] However, in Fe-Cu model alloys, a long lifetime component of $\sim$300 ps of positron annihilation is detected[5] suggesting the stabilization of such small vacancy clusters by Cu impurity atoms.

In this paper, we study the details of the structure and the binding energies of vacancy-Cu clusters of various sizes in α-Fe. In this study, atomic-scale computer simulations such as molecular-dynamics (MD) and lattice Monte Carlo (LMC) methods are used in order to provide detailed information that would help the interpretation of the above-mentioned experimental observations. Energy-minimum structures of vacancy-Cu clusters with given numbers of vacancies and Cu atoms are determined. The binding energies of a vacancy and a Cu to the vacancy-Cu clusters are also calculated from the formation energies of such energy-minimum clusters. We develop equations that describe the formation and binding energies of vacancy-Cu clusters as a function of the numbers of vacancies and Cu atoms. The implications of the results are discussed.

II. SIMULATION METHOD

A LMC computer-simulation method following the Metropolis algorithm[7] is used to search for energy-minimum

atomic structures of vacancy-Cu clusters. Initially, a given number of vacancies and Cu atoms are randomly located at the lattice sites of a computation box with a size of $15\times15\times15a_0$, where a_0 is a lattice unit. Then, any two out of the vacancies and Cu atoms are randomly picked up to calculate the crystal energy change due to the position exchange of the two. If the energy becomes lower by the position exchange, the new configuration is adopted. If not, the new configuration is adopted with the probability of the Boltzmann's factor, $\exp(-\Delta E/kT)$, where ΔE is the crystal energy change, k the Boltzmann's constant, and T the crystal temperature, respectively. This process, i.e., one LMC step, is repeated until the minimum crystal energy is reached. The crystal temperature is initially set to 600 K, and then it is decreased by 5 K at every 100 LMC steps (simulated annealing). After the LMC calculation is completed, the positions of Fe and Cu atoms, which are fixed at lattice sites of the computation box during the LMC calculation, are relaxed by MD using a numerical quenching algorithm in order to calculate the final crystal energy. In both LMC and MD calculations, the Finnis-Sinclair-type interatomic potential for Fe-Cu alloy developed by Ackland *et al.*[8] is used. Ideally, MD quenching calculation may need to be performed after each LMC step. We tested this, and confirmed that both approaches, MD quenching after every LMC step and one MD quenching after LMC minimization is completed, give the same results.

III. PURE-VACANCY CLUSTERS AND PURE-CU CLUSTERS IN α-FE

The energy-minimum structures for pure-vacancy clusters and pure-Cu clusters and their formation and binding energies in α-Fe are calculated for the clusters of up to 100 in size. The energy-minimum structures of pure-vacancy clusters are, in general, spherical in shape in good agreement with the compact configuration by Beeler[9] and also the results by Soneda and Diaz de la Rubia *et al.*[10] No collapse of a vacancy cluster to a dislocation loop took place. The structure of pure-Cu clusters is also spherical in shape. However, since Cu is an oversized element compared to Fe, and its intrinsic crystal structure is fcc, there should be a nontrivial strain field. This will be discussed later.

Figure 1 shows the formation energies of vacancy clusters, $E_f^{vac}(n)$, and Cu clusters, $E_f^{Cu}(n)$, whose definitions are given as

$$E_f^{vac}(n_{vac}) = m\times E_{coh}^{Fe} - [E_c^{vac}(m,n_{vac}) + n_{vac}\times E_{coh}^{Fe}] \quad (1)$$

and

$$E_f^{Cu}(n_{Cu}) = (m\times E_{coh}^{Fe} + n_{Cu}\times E_{coh}^{Cu}) - [E_c^{Cu}(m,n_{Cu}) + n_{Cu}\times E_{coh}^{Fe}], \quad (2)$$

where, m, n_{vac} and n_{Cu} are the numbers of lattice sites in the computation model crystal, vacancies, and Cu atoms, respectively, E_{coh}^{Fe} and E_{coh}^{Cu} are the cohesive energies of α-Fe and fcc Cu, respectively, and $E_c^{vac}(m,n_{vac})$ and $E_c^{Cu}(m,n_{Cu})$ are an Fe crystal energy with m lattice sites including n_{vac} vacancies and n_{Cu} Cu atoms, respectively. The monovacancy formation energy obtained here is 1.71 eV, and is in good agreement with experimental values of 1.79 eV (Ref. 11) and 1.85 eV,[12] and the MD results of 1.73 eV using different embedded atom method (EAM) potentials,[10] as well as first-principles calculation of 1.9 eV.[13] The substitutional energy of a single Cu atom is 0.29 eV in this study, which is slightly smaller than the first-principles calculation result of 0.45 eV.[14] Regarding the terminology, $E_f^{Cu}(1)$ should be a ''substitutional'' energy of a Cu atom rather than a ''formation'' energy. However, we use hereafter a unified wording of ''formation'' energy for simplicity.

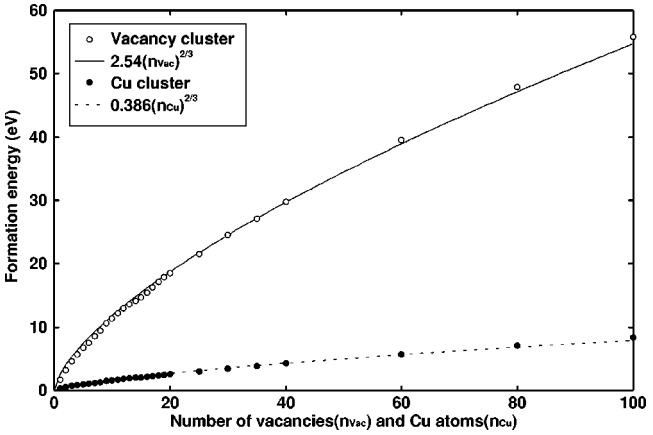

FIG. 1. Formation energies of pure-vacancy and pure-Cu clusters. The circles show the formation energies obtained by MD, and the lines show the approximations of the energies by Eqs. (3) and (4) (see text). Both equations have the same exponent suggesting almost the same structure of vacancy and Cu clusters.

It is useful to find equations that describe the formation energies of pure-vacancy and pure-Cu atom clusters. We found that the formation energies are well described by the following equations as indicated in Fig. 1:

$$E_f^{vac}(n_{vac}) = 2.54(n_{vac})^{2/3} \quad (3)$$

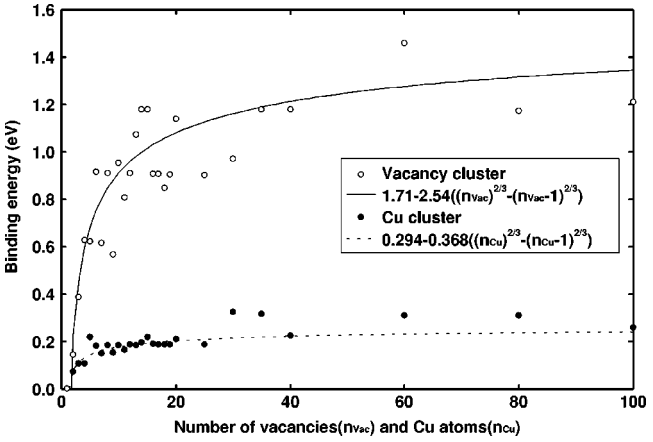

FIG. 2. Binding energies of pure-vacancy and pure-Cu clusters. The circles show the binding energies calculated as the difference of the formation energies obtained by MD, and the lines are those calculated using the Eqs. (7) and (8) (see text). The equations well describe the calculated energies.

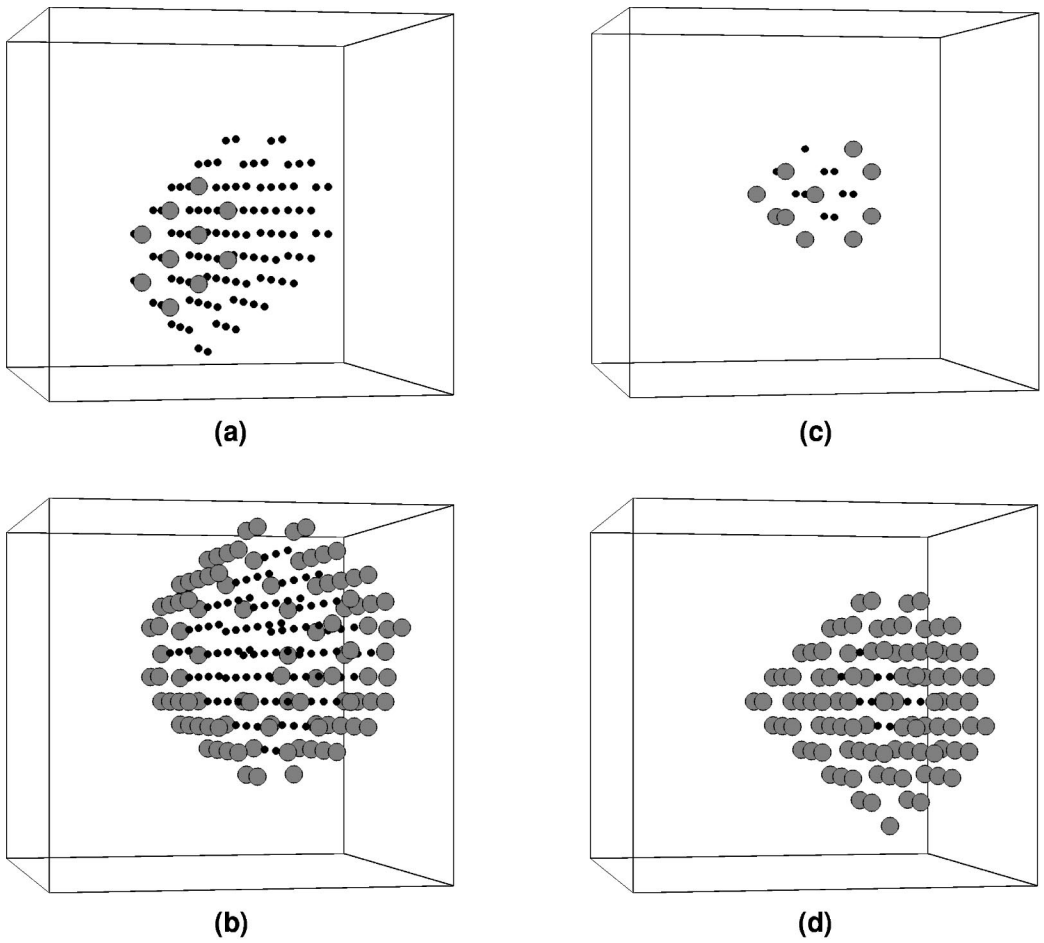

FIG. 3. Energy-minimum structures of vacancy-Cu clusters. The black circles are vacancies, and the gray circles are Cu atoms. The clusters include (a) 100 vacancies and 10 Cu atoms, (b) 100 vacancies and 100 Cu atoms, (c) 10 vacancies and 10 Cu atoms, and (d) 10 vacancies and 100 Cu atoms.

and

$$E_f^{Cu}(n_{Cu}) = 0.368(n_{Cu})^{2/3}. \quad (4)$$

The binding energies of vacancy clusters, $E_b^{vac}(n_{vac})$, and Cu clusters, $E_b^{Cu}(n_{Cu})$, are defined as

$$E_b^{vac}(n_{vac}) = E_f^{vac}(n_{vac}-1) + E_f^{vac}(1) - E_f^{vac}(n_{vac}) \quad (5)$$

and

$$E_b^{Cu}(n_{Cu}) = E_f^{Cu}(n_{Cu}-1) + E_f^{Cu}(1) - E_f^{Cu}(n_{Cu}). \quad (6)$$

We obtained the binding energies of these clusters for the sizes up to 100 by calculating all the formation energies necessary to apply the definitions (5) and (6) by MD and LMC. For example, we calculated $E_f^{vac}(100)$ and $E_f^{vac}(99)$ to obtain $E_b^{vac}(100)$. The calculated binding energies are shown in Fig. 2. The binding energies can also be calculated by substituting Eqs. (3) and (4) into Eqs. (5) and (6) as

$$E_b^{vac}(n_{vac}) = 1.71 - 2.54[(n_{vac})^{2/3} - (n_{vac}-1)^{2/3}] \quad (7)$$

and

$$E_b^{Cu}(n_{Cu}) = 0.294 - 0.368[(n_{Cu})^{2/3} - (n_{Cu}-1)^{2/3}]. \quad (8)$$

Here we used MD results rather than Eqs. (3) and (4) for the values of $E_f^{vac}(1)$ and $E_f^{Cu}(1)$ of Eqs. (5) and (6). These estimations are also plotted in Fig. 2 with lines showing good approximation of the circles. The results of the formation and binding energies of the vacancy clusters are very consistent with the previous results by Soneda and Diaz de la Rubia,[10] who used a different EAM-type interatomic potential[15] from the one used in this study.

IV. VACANCY-CU CLUSTERS

Energy-minimum structures of vacancy-Cu clusters in α-Fe are calculated. Both the number of vacancies and the number of Cu atoms in a cluster range from 1 to 100 in our calculation matrix to obtain detailed information on the characteristics of vacancy-Cu clusters.

Figures 3(a)–3(d) show typical structures of vacancy-Cu clusters, where the cluster compositions are [Fig. 3(a)] 100 vacancies and 10 Cu atoms, [Fig. 3(b)] 100 vacancies and 100 Cu atoms, [Fig. 3(c)] 10 vacancies and 10 Cu atoms, and [Fig. 3(d)] 10 vacancies and 100 Cu atoms, respectively. General observations we noted throughout all the results are as follows. First, vacancies form a cluster at the center of the vacancy-Cu cluster and we call this hereafter a *central va-*

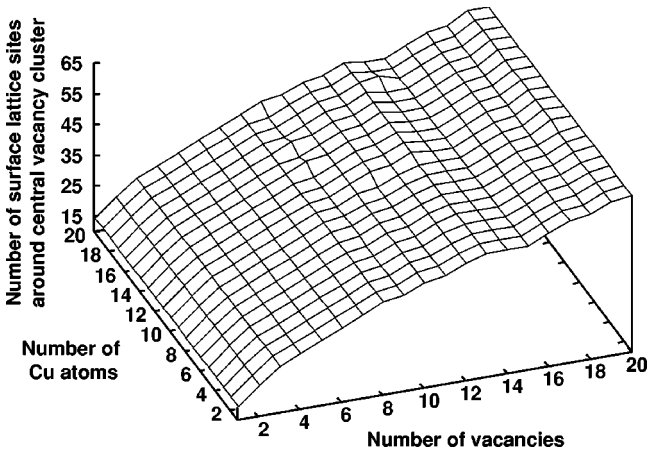

FIG. 4. Number of surface lattice sites of the central vacancy clusters. The surface lattice sites are defined as the sites located within the second-nearest-neighbor distance from the central vacancy cluster.

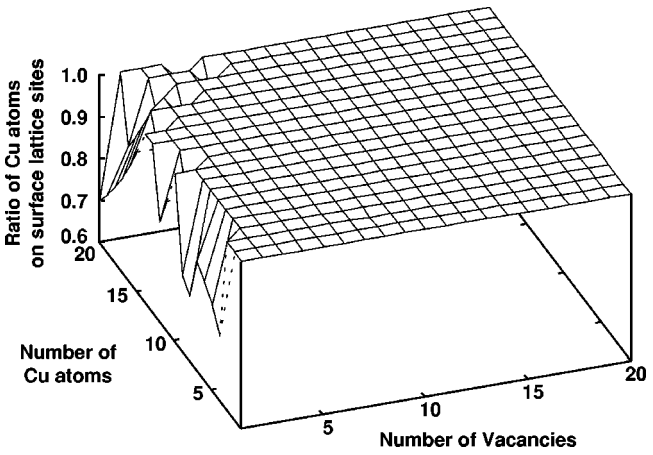

FIG. 5. Ratio of the number of Cu atoms located on the surface lattice sites to the total number of Cu atoms. Unity means that all the Cu atoms sit on the surface of the central vacancy cluster. In some cases when the size of the vacancy cluster is small, the sites within the third-nearest-neighbor distance are more preferable than the surface lattice sites even though there are still some surface lattice sites available.

cancy cluster, whose configuration does not change very much when the number of Cu atoms changes. The configuration of the central vacancy cluster is almost identical to that of the pure vacancy cluster with the same number of vacancies in α-Fe. This can be seen when one compares Figs. 3(a) and 3(b), and Figs. 3(c) and 3(d). Figure 4 further shows this situation, where the number of atoms within the second-nearest-neighbor distance from the central vacancy clusters (we call this hereafter *surface lattice sites*) is plotted as a function of the numbers of vacancies and Cu atoms. One can see that the number of the surface lattice sites increases as the number of vacancies increases, but is almost independent of the number of Cu atoms. This means that the morphology of the central vacancy clusters is not largely affected and changed by the Cu atoms.

Secondly, Cu atoms tend to sit on the surface of the central vacancy clusters as can be seen in Figs. 3(a)–3(d). Figure 5 shows the ratio of the number of Cu atoms that sit at the surface lattice sites of the central vacancy cluster to the total number of Cu atoms. The ratio is always unity except for the cases where the number of vacancies is small, indicating that all the Cu atoms sit at the surface lattice sites when there are a sufficient number of surface lattice sites available. In addition, when the number of Cu atoms is much smaller than that of the surface lattice sites, Cu atoms tend to agglomerate locally on the surface of the central vacancy cluster as shown in Fig. 3(a), rather than occupy isolated surface lattice sites. In other words, local coating of the surface of the central vacancy cluster takes place when the number of Cu atoms is smaller than the surface lattice sites. On the other hand, when the number of Cu atoms is much larger than that of the vacancies, the whole surface of the central vacancy cluster is coated by Cu atoms, and the central vacancy cluster is buried in a shell of Cu atoms as shown in Fig. 3(d).

Next, we calculated formation energies of vacancy-Cu clusters defined as

$$E_f^{vac\text{-}Cu}(n_{vac},n_{Cu}) = (m\times E_{coh}^{Fe} + n_{Cu}\times E_{coh}^{Cu}) - [E_c^{vac\text{-}Cu}(m,n_{vac},n_{Cu}) + (n_{vac}+n_{Cu})\times E_{coh}^{Fe}], \quad (9)$$

where $E_f^{vac\text{-}Cu}(n_{vac},n_{Cu})$ is the formation energy of the cluster containing n_{vac} vacancies and n_{Cu} Cu atoms, m is the number of lattice sites in the computation crystal, $E_c^{vac\text{-}Cu}(m,n_{vac},n_{Cu})$ is the energy of the crystal containing m lattice sites, n_{vac} is the vacancies, and n_{Cu} is the Cu atoms, respectively. We calculated all the formation energies of the vacancy-Cu clusters containing less than 20 vacancies and 20 Cu atoms. For larger vacancy-Cu clusters, we calculated the formation energies for selected sizes of the clusters. The largest cluster calculated consists of 100 vacancies and 100 Cu atoms. Then, we developed an equation describing the formation energy as a function of the numbers of vacancies and Cu atoms. Such an equation should help us in understanding the general characteristics of the formation energy of vacancy-Cu clusters.

For the equation development, we first examined the difference between the formation energies of vacancy-Cu clusters and pure-Cu clusters containing the same number of Cu atoms. In Fig. 6, where the energy differences are plotted as a function of the number of Cu atoms for various numbers of vacancies, we can see two things: (i) the energy difference is a monotonically decreasing function of the number of Cu atoms when the number of Cu atoms is smaller than a certain number we call the *cutoff* number, and (ii) above the cutoff number, the energy difference tends to saturate to a lowest value. From a regression analysis, we found that a quadratic function of the number of Cu atoms well describes the decreasing part of the energy difference as shown in Fig. 8 below. We obtained an equation to describe the formation energy of the vacancy-Cu clusters as

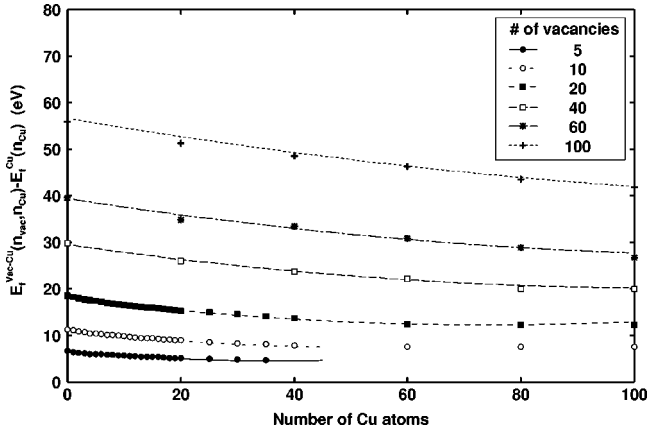

FIG. 6. Difference of the formation energy of a vacancy-Cu cluster and a pure-Cu cluster containing the same number of Cu atoms. Symbols are well described by the quadratic functions of the number of vacancies indicated by lines. One can see, for example, in the case of 10 vacancies, that the energy difference reaches a constant value when the number of Cu atoms is larger than 60 suggesting an idea of a cutoff number.

$$E_f^{vac\text{-}Cu}(n_{vac},n_{Cu}) = E_f^{Cu}(n_{Cu}) + A(n_{vac}) + B(n_{vac}) \times (C(n_{vac}) - n_{Cu})^2, \tag{10}$$

where the terms, *A*, *B*, and *C*, are determined as functions of the number of vacancies as follows:

$$A(n_{vac}) = 1.43(n_{vac})^{0.72}, \tag{11}$$

$$B(n_{vac}) = \begin{cases} 0.002\,80(n_{vac})^{-0.33} & \text{when } C(n_{vac}) > n_{Cu}, \\ 0 & \text{when } C(n_{vac}) \leqslant n_{Cu}, \end{cases} \tag{12}$$

and

$$C(n_{vac}) = 16.1(n_{vac})^{0.51}. \tag{13}$$

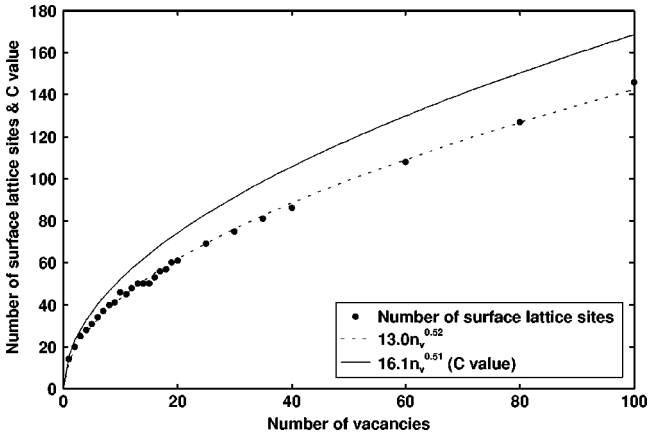

FIG. 7. Comparison between the *C* value of Eq. (13) and the number of surface lattice sites. The number of surface lattice sites is approximated by the broken line. Both curves have the same exponent of about 0.5 indicating that the *C* value, i.e., the cutoff number, is strongly related to the number of surface lattice sites.

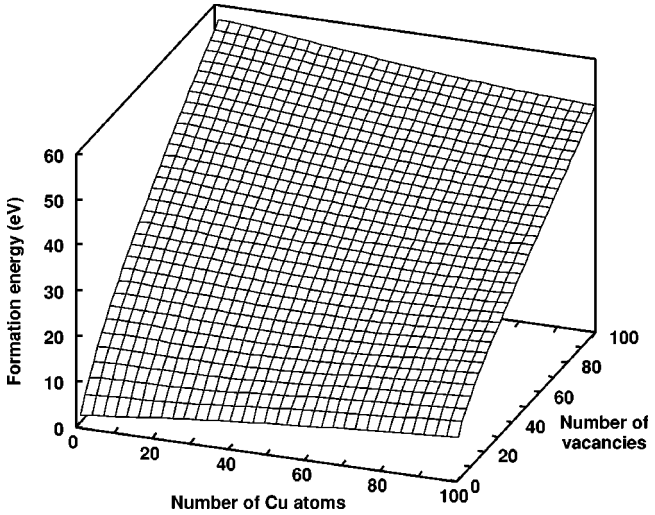

FIG. 8. Formation energies of vacancy-Cu clusters calculated by Eqs. (10)–(13).

The function *C* is the cutoff number of Cu atoms. We found that the *C* value has a strong correlation with the number of surface lattice sites as shown in Fig. 7. The number of the surface lattice sites, n_{sls}, is approximated by the following equation:

$$n_{sls} = 13.0(n_{vac})^{0.52} \tag{14}$$

as shown by the dotted line in Fig. 7. This equation has the same exponent as that of Eq. (13) indicating that the *C* value is always 24% larger than the number of the surface lattice sites. In order to check the accuracy of Eqs. (10)–(13), we compared the formation energies of vacancy-Cu clusters calculated from the above equations with those calculated by Monte Carlo (MC) and MD as shown in Fig. 8. We can see that the equations describe the formation energies with acceptable accuracy. Figure 9 shows the formation energy of

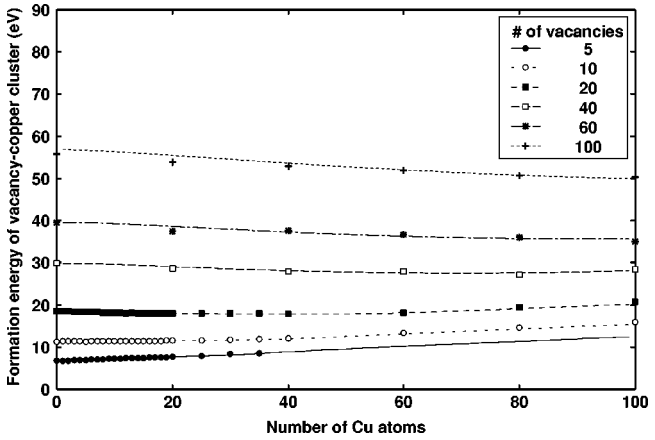

FIG. 9. Formation energies of vacancy-Cu clusters as a function of the numbers of vacancies and Cu atoms. The lines are the slices of Fig. 8 taken at the fixed numbers of vacancies such as 5, 10, 20, 40, 60, and 100. When the number of vacancies is small, the formation energy increases as the number of Cu atoms increases. When the number of vacancies is large, the formation energy decreases as the number of Cu atoms increases.

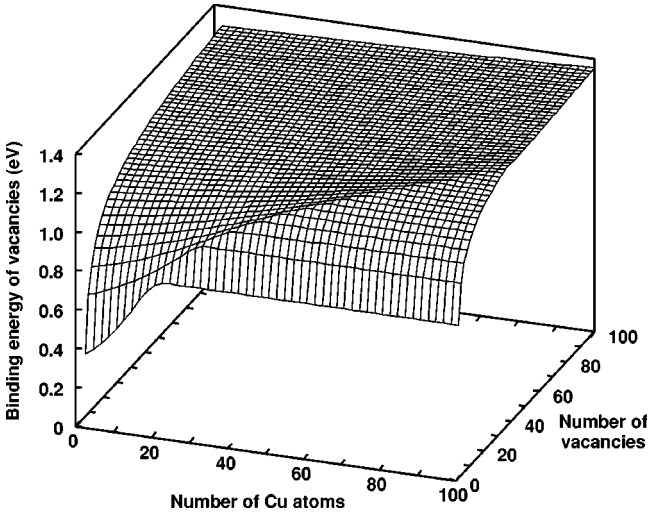

FIG. 10. Binding energies of a vacancy to the vacancy-Cu clusters calculated by Eqs. (10)–(13) and (15). The idea of the cutoff number, *C*, of the formation energy makes the vacancy binding energy constant when the number of Cu atoms is larger than the cutoff number.

vacancy-Cu clusters as a function of the numbers of Cu atoms and vacancies obtained from Eqs. (10)–(13).

The binding energies of a vacancy or a Cu atom to the vacancy-Cu clusters are calculated using the following equations:

$$E_b^{vac\text{-}Cu,vac}(n_{vac},n_{Cu}) = E_f^{vac\text{-}Cu}(n_{vac}-1,n_{Cu}) + E_f^{vac}(1) - E_f^{vac\text{-}Cu}(n_{vac},n_{Cu}) \tag{15}$$

and

$$E_b^{vac\text{-}Cu,Cu}(n_{vac},n_{Cu}) = E_f^{vac\text{-}Cu}(n_{vac},n_{Cu}-1) + E_f^{Cu}(1) - E_f^{vac\text{-}Cu}(n_{vac},n_{Cu}). \tag{16}$$

We obtained the binding energies using the values obtained by the present calculations. We can also calculate those values by substituting Eqs. (10)–(13) into Eqs. (15) and (16). The results are shown in Figs. 10 and 12 below. Regarding the vacancy binding energies, it is interesting to see in Fig. 10 that the vacancy binding energy becomes constant against the number of Cu atoms when the cutoff condition of $16.1(n_{vac})^{0.51} < n_{Cu}$ is met. This is further confirmed by comparing the binding energies obtained by the present calculations and Fig. 10 as shown in Fig. 11, where the vacancy binding energy saturates when the number of Cu atoms is larger than about 50. This means that when the condition of $16.1(n_{vac})^{0.51} < n_{Cu}$ is met, additional Cu atoms have no interaction with the central vacancy clusters.

Regarding the Cu binding energies, on the other hand, we can see in Fig. 12 that the binding energy reaches a maximum at a certain number of Cu atoms. Beyond that number of Cu atoms, the binding energy decreases down to the Cu binding energy of pure-Cu clusters. Cu binding energy increases rapidly as the number of vacancies increases to reach values larger than the solution energy of 0.29 eV. These results indicate that a pure Cu cluster is stabilized when it exists with vacancies. At the same time, however, we also need to be aware that the absolute magnitude of the Cu binding energies is no larger than about 0.4 eV for the clusters examined.

In order to investigate the origin of the stabilization of Cu binding to vacancy-Cu clusters, we looked at the atomic arrangements of a pure-Cu cluster, a vacancy-Cu cluster, and a pure-vacancy cluster as show in Figs. 13(a)–13(c), respec-

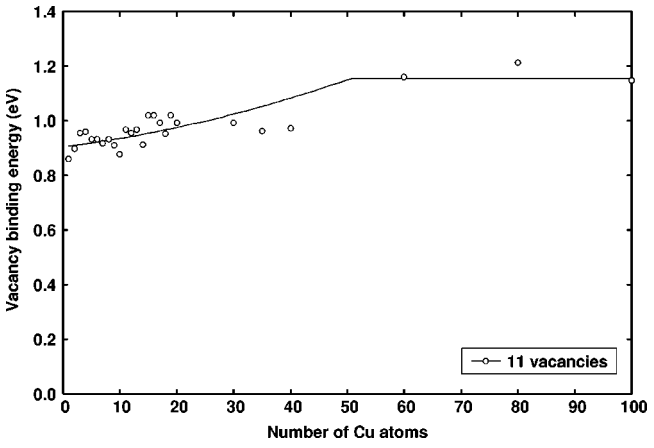

FIG. 11. Detailed comparison of the vacancy binding energies calculated by MD and by Eqs. (10)–(13) and (15). The line is a slice of Fig. 10 taken at 11 vacancies. A tendency can be seen in which the binding energy reaches a constant value when the number of Cu atoms is larger than 50.

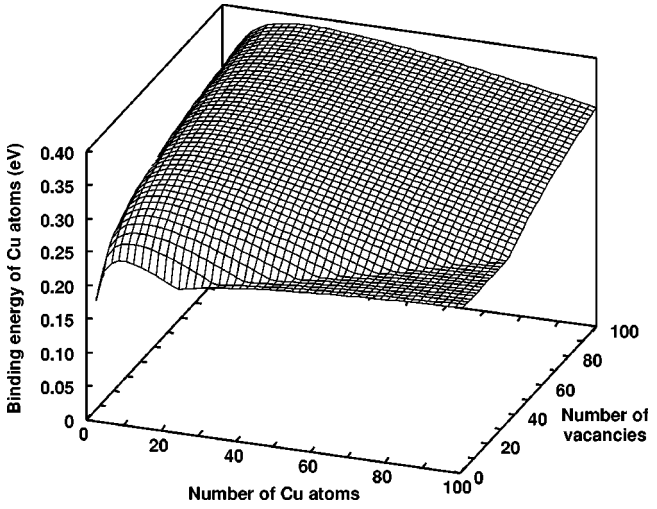

FIG. 12. Binding energies of the Cu atom to the vacancy-Cu clusters calculated by Eqs. (10)–(13) and (16). The binding energy reaches a maximum as the number of Cu atoms increases. When the number of Cu atoms is sufficiently larger than the number of vacancies, the binding energy becomes identical to that of the pure-Cu cluster.

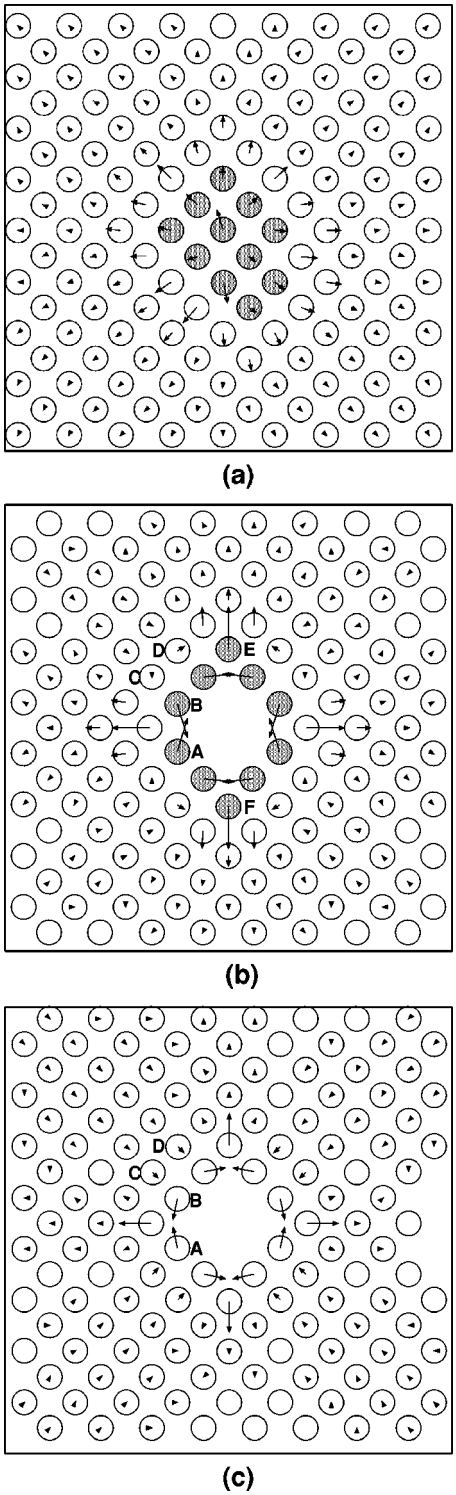

FIG. 13. Displacement field of atoms around (a) a pure-Cu cluster, (b) a vacancy-Cu cluster, and (c) a pure-vacancy cluster. Atoms on the adjacent two (100) planes are displayed. The numbers of Cu atoms and vacancies are 20 and 4, respectively. Open circles are Fe atoms, and gray circles are Cu atoms. Bars starting from the center of the circles show the displacement vector. The amount of displacement is magnified.

tively. The plots show the atom positions on the (100) plane. Gray circles are Cu atoms, and the other circles represent Fe atoms. The number of Cu atoms is 20, and the number of vacancies is four. A bar starting from a center of an atom circle indicates a displacement vector of the atom. Since a Cu atom is an oversized atom in the Fe matrix, a repulsive force acts on the Cu atoms resulting in the swelling of the Cu area as shown in Fig. 13(a). However, when the cluster has vacancies at its center, some Cu atoms adjacent to the vacancies can relax inward to reduce the strain around the cluster as can be seen in Fig. 13(b). The relaxation details of the vacancy-Cu cluster and the vacancy cluster are different in Figs. 13(b) and 13(c). The Cu atoms labeled as ''A'' and ''B'' in Fig. 13(b) show clear displacements in an inward direction, while the corresponding Fe atoms labeled ''A'' and ''B'' in Fig. 13(c) do not show such a tendency. On the other hand, the Fe atoms labeled ''C'' and ''D'' in Fig. 13 (c) show inward displacement while corresponding Fe atoms also labeled ''C'' and ''D'' in Fig. 13(b) show very different displacement. It is interesting to discuss the symmetry of the vacancy-Cu cluster of Fig. 13(b). We chose 20 Cu atoms for the demonstration in Fig. 13, because 20 is the number of the lattice sites located within the first-nearest-neighbor distance from the vacancy cluster. We expected that all the Cu atoms sit on such lattice sites. However the resulting structure shows that four Cu atoms, two of which are labeled ''E'' and ''F'' in Fig. 13(b), chose lattice sites located with in the second-nearest-neighbor distance from the vacancy cluster rather than the sites within the first-nearest-neighbor distance.

The results obtained in this section can be summarized as follows. Compared with the Fe atom, the Cu atom is the oversized atom. When the number of Cu atoms is sufficiently larger than that of the surface lattice sites of the central vacancy cluster as shown in Fig. 3(d), the growth of the central vacancy cluster is almost equivalent to the growth of the pure-vacancy cluster in the bcc-Cu crystal having the Fe lattice unit. This is reflected in Eq. (13), where the function has the same form and almost the same exponent value as those of Eq. (14) obtained for the vacancy cluster in α-Fe. The growth of the outer Cu shell around the central vacancy cluster is effectively identical to the growth of pure Cu clusters in α-Fe. In these cases, the formation energy is a simple sum of those of the outer Cu shell and the central vacancy cluster, and there is no synergetic term between the Cu atoms and vacancies in the formation energy. On the other hand, when the condition $16.1(n_{vac})^{0.51}<n_{Cu}$, i.e., $C(n_{vac})<n_{Cu}$ is met as shown in Fig. 13(a), a new term, $B(n_{vac})(C(n_{vac})-n_{Cu})^2$, arises indicating that the synergetic effect between the Cu atoms and vacancies is no longer negligible. Considering the fact that the value of $C(n_{vac})$ is close to the number of the surface lattice sites of the central vacancy clusters, see Fig. 7, the term means that the magnitude of the synergetic effect is a function of the surface lattice sites not occupied by Cu atoms. It is caused by the size difference between the Cu and Fe atoms. Compared with the size of the Fe atom, the Cu atom is the slightly oversized atom, therefore Cu atoms and their clusters tend to swell in the α-Fe matrix. When the number of Cu atoms is larger than the number

$16.1(n_{vac})^{0.51} < n_{Cu}$, then swelling of the Cu shells cannot occur. However, if the number of Cu atoms is smaller than the equation, the swelling can occur.

V. DISCUSSION

The primary concern of this paper is to study the vacancy-Cu clusters in α-Fe, in terms of the structure of the clusters and the binding energies of a vacancy and a Cu atom to the clusters. Our MD and MC calculations demonstrate that, in general, the clusters consist of a central vacancy cluster decorated, or coated, by Cu atoms.

The structure of a central vacancy cluster buried in a Cu shell is consistent with experimental observations. Nagai *et al.*[5] measured the lifetimes and the momentum spectra of the gamma rays emitted by the annihilation of positrons in neutron-irradiated Fe-1.3 wt %-Cu model alloys using a conventional lifetime measurement technique and a sophisticated coincidence Doppler broadening technique of positron annihilation experiments. Their results show that vacancy-type defects having long lifetimes are produced during the neutron irradiation, and furthermore the high-momentum spectra of the annihilation gamma rays are almost identical to those for pure-Cu crystals. Their interpretation is that the atoms that sit on the surface of the vacancy clusters induced in the materials by the neutron irradiation are all Cu atoms. This is consistent with our computer-simulation results of stable vacancy-Cu clusters.

The strengthening of the binding of a Cu atom and a vacancy to small vacancy-Cu clusters should affect the microstructure evolution in irradiated Fe-Cu crystals and Cu containing RPV materials. Before discussing the Fe-Cu system, it should be worthwhile reviewing the current understanding of the vacancy formation in pure Fe. Postirradiation isochronal annealing and resistivity measurement studies of high-purity Fe irradiated by electrons at a low temperature shows that the stage-V temperature for vacancies is thermally unstable between 500 K and 600 K.[16] On the other hand, in the pure Fe irradiated by neutrons at 100 °C, small vacancy clusters of $\sim$9 to 14 vacancies are formed after irradiation.[6] These small vacancy clusters shrink in size as the annealing temperature increases to form larger voids or they annihilate at sinks. Beyond the stage-V temperatures, such small vacancy clusters evaporate, and only a small fraction of voids, which also continue to evaporate, remains. Recent TEM study[17] of Fe irradiated at 310 K by neutrons shows consistent results in that almost all the microstructures resolved by the TEM technique are interstitial-type dislocation loops, and no vacancy-type defect is observed. Molecular-dynamics studies support these observations. MD studies of displacement cascades in Fe (Refs. 10, and 18–20) have shown that the clear clustering of vacancies does not take place at the end of the cooling phase of the cascades in sharp contrast to the fcc metals.[21,22] The binding energies of small vacancy clusters of $\sim$10 members calculated by molecular dynamics[10] are $\sim$0.5 eV, which will be sufficient to be stable at $\sim$400 K but not at higher temperatures. Thus, these results give us the following picture of vacancy cluster formation and stability in α-Fe. Displacement cascades do not produce vacancy clusters directly. Vacancies introduced by cascades form clusters by primarily agglomerating in small regions, but such formed clusters are not stable at temperatures around stage V, which is close to the RPV operation temperature of 563 K.

In the Fe-Cu system, the present work suggests that the vacancy-Cu clusters are more stable than pure-vacancy and pure-Cu clusters of the same size, and this effect is significant when the numbers of vacancies and Cu atoms are small. Although the calculated binding energies of small vacancy-Cu clusters are not sufficiently large to survive dissociation at the stage-V temperature of pure Fe, a large increase in binding energy should make the lifetime of the vacancy-Cu clusters much longer.[23] This effect should certainly increase the chance of cluster growth, and should promote the vacancy-Cu cluster growth. In addition, it should be pointed out that this lifetime change may cause a different dose rate dependence of the damage evolution in Fe-Cu crystals from that in pure-Fe crystals.

Finally, we would like to discuss the dissociation process of vacancy-Cu clusters. This is important when we apply a technique such as the kinetic Monte Carlo method[10,24] to the calculation of microstructure evolution under irradiation. Evaporation of Cu atoms from the cluster should be somewhat straightforward. Cu atoms will be taken away from the interface of the cluster and the Fe matrix by vacancies. In this case, the dissociation energy should be a simple sum of the binding energy of the Cu atom and the migration energy of the vacancy. Of course, it should be noted that there is another chance for a vacancy as a carrier of Cu atoms to be absorbed by the vacancy-Cu cluster when the vacancy comes within a certain distance from the cluster. This will affect the prefactor of the dissociation process, and further information needs to be provided by such techniques as molecular dynamics.

On the other hand, dissociation of a vacancy from a vacancy-Cu cluster is complicated especially when the vacancy cluster is buried in a thick Cu shell as shown in Fig. 3(d). The vacancy binding energy that we calculated in this paper is the energy difference between the crystals containing (i) n-vacancy and m-Cu clusters and (ii) $(n-1)$-vacancy and m-Cu clusters plus one isolated vacancy. However, in such a case as Fig. 3(d), a vacancy on the surface of the central vacancy cluster needs to dissociate from this internal vacancy cluster first, make several jumps in the Cu shell, and then escape from the surface of the vacancy-Cu cluster. Clearly this is a multiprocess event, and not only the activation energy but also the prefactor of the event should be very affected.

VI. CONCLUSIONS

Structures and energies of vacancy-Cu clusters in α-Fe were studied by means of atomistic-scale computer-simulation techniques such as the molecular-dynamics and the Monte Carlo techniques. In general, the cluster consists of a vacancy cluster buried at the center of the surrounding Cu shell. This structure is consistent with information obtained by the coincidence Doppler broadening measurement of positron annihilation. When the number of Cu atoms is not sufficiently large to cover the whole surface of the central vacancy cluster, the Cu atoms segregate locally on the sur-

face instead of sitting at the separated lattice sites to each other.

An equation was developed that describes the formation energy of the vacancy-Cu clusters. The equation consists of a Cu clustering term, a vacancy clustering term, and a synergetic term of vacancy-Cu interaction. The synergetic term is related to the number of surface lattice sites of the central vacancy cluster not occupied by Cu atoms.

The binding energies of a vacancy and a Cu atom to the vacancy-Cu clusters were calculated from the formation energies. Cu atoms enhance the binding of a vacancy to the vacancy-Cu clusters and this is more efficient when the number of vacancies is small. Vacancies also enhance the binding of a Cu atom to the vacancy-Cu clusters. For a given number of vacancies, the binding energy reaches a maximum at a relatively small number of Cu atoms, and it approaches the Cu binding energy of the pure-Cu cluster when the number of Cu atoms increases.

[1] G. R. Odette and G. E. Lucas, Radiat. Eff. Defects Solids **144**, 189 (1998).
[2] P. Pareige and M. K. Miller, Appl. Surf. Sci. **94/95**, 370 (1996).
[3] R. G. Carter, N. Soneda, K. Dohi, J. M. Hyde, C. A. English, and W. L. Server, J. Nucl. Mater. **298**, 211 (2001).
[4] P. Pareige, R. E. Stoller, K. F. Russel, and M. K. Miller, J. Nucl. Mater. **249**, 165 (1997).
[5] Y. Nagai, Z. Tang, M. Hasegawa, T. Kanai, and M. Saneyasu, Phys. Rev. B **63**, 134110 (2001).
[6] M. Eldrup and B. N. Singh, J. Nucl. Mater. **276**, 269 (2000).
[7] M. Metropolis, A. W. Rosenbluth, A. H. Teller, and E. Teller, J. Chem. Phys. **21**, 1087 (1953).
[8] G. J. Ackland, D. J. Bacon, and T. Harry, Philos. Mag. A **75**, 713 (1997).
[9] J. R. Beeler, *Radiation Effects Computer Experiments* (North-Holland, Amsterdam, 1983).
[10] N. Soneda and T. Diaz de la Rubia, Philos. Mag. A **78**, 995 (1998).
[11] L. D. Schepper, D. Segers, L. Dorikens-Vanpraet, M. Dorikens, G. Knuyt, L. M. Stals, and P. Moser, Phys. Rev. B **27**, 5257 (1983).
[12] Y. Shirai, H. E. Schaefer, and A. Seeger, in *Proceedings of the Eighth International Conference On Positron Annihilation*, edited by L. Dorikens-Vanpraet, M. Dorikens, and D. Segers (World Scientific, Singapore, 1988).
[13] T. Ohnuma and N. Soneda (unpublished).
[14] C. Domain and C. S. Becquart, Phys. Rev. B **65**, 024103 (2002).
[15] R. A. Johnson and D. J. Oh, J. Mater. Res. **4**, 1195 (1989).
[16] S. Takaki, J. Fuss, H. Kugler, U. Dedek, and H. Schultz, Radiat. Eff. **79**, 87 (1983).
[17] M. Victoria, N. Baluc, C. Bailat, Y. Dai, M. I. Luppo, R. Shaublin, and B. N. Singh, J. Nucl. Mater. **276**, 114 (2000).
[18] A. F. Calder and D. J. Bacon, J. Nucl. Mater. **207**, 25 (1993).
[19] W. J. Phythian, R. E. Stoller, A. J. E. Foreman, A. F. Calder, and B. J. Bacon, J. Nucl. Mater. **223**, 245 (1995).
[20] R. E. Stoller, J. Nucl. Mater. **276,** 22 (2000)..
[21] T. Diaz de la Rubia and M. W. Guinan, Phys. Rev. Lett. **66**, 2766 (1991).
[22] M. J. Caturla, M. Wall, E. Alonso, T. Diaz de la Rubia, T. Felter, and M. J. Fluss, J. Nucl. Mater. **276**, 186 (2000).
[23] B. D. Wirth and G. R. Odette, Mater. Res. Soc. Symp. Proc. **540**, 637 (1999).
[24] M. Jaraiz, G. H. Gilmer, J. M. Poate, and T. Diaz de la Rubia, Appl. Phys. Lett. **68**, 409 (1996).